The EMBO Journal (2009) 28, 2677–2685 | © 2009 European Molecular Biology Organization | All Rights Reserved 0261-4189/09
www.embojournal.org

THE EMBO JOURNAL

Structural basis of GDP release and gating in G protein coupled Fe^{2+} transport

Amy Guilfoyle[1,5], Megan J Maher[1,5], Mikaela Rapp[1,6], Ronald Clarke[2], Stephen Harrop[3] and Mika Jormakka[1,4,*]

[1]Structural Biology Program, Centenary Institute, Sydney, New South Wales, Australia, [2]School of Chemistry, University of Sydney, Sydney, New South Wales, Australia, [3]Department of Biophysics, University of New South Wales, Sydney, New South Wales, Australia and [4]Faculty of Medicine, Central Clinical School, University of Sydney, Sydney, New South Wales, Australia

G proteins are key molecular switches in the regulation of membrane protein function and signal transduction. The prokaryotic membrane protein FeoB is involved in G protein coupled Fe^{2+} transport, and is unique in that the G protein is directly tethered to the membrane domain. Here, we report the structure of the soluble domain of FeoB, including the G protein domain, and its assembly into an unexpected trimer. Comparisons between nucleotide free and liganded structures reveal the closed and open state of a central cytoplasmic pore, respectively. In addition, these data provide the first observation of a conformational switch in the nucleotide-binding G5 motif, defining the structural basis for GDP release. From these results, structural parallels are drawn to eukaryotic G protein coupled membrane processes.

The EMBO Journal (2009) **28,** 2677–2685. doi:10.1038/emboj.2009.208; Published online 23 July 2009
Subject Categories: signal transduction; structural biology
Keywords: crystallography; GDP release; GTPase; iron transport

Introduction

The nucleotide GTP and its cognate GTPases (G proteins) are critical for normal physiology in all organisms by acting as molecular 'on' (GTP bound) or 'off' (GDP bound) switches for fundamental cellular processes, such as protein synthesis and sorting, cell growth, and regulation of ion channels (Cachero *et al*, 1998; Finlin *et al*, 2006). As such, their aberrant functions have resulted in a number of pathophysiological disorders, such as asthma and cancer (Karnoub and Weinberg, 2008; Schaafsma *et al*, 2008). Structural studies have anatomically characterized G proteins, revealing a highly conserved GTP-binding domain of roughly 160 residues distinguished by five short amino-acid motifs, termed G1–G5, that are critical in the binding of both a magnesium (Mg^{2+}) ion and the guanine nucleotide (Sprang, 1997; Vetter and Wittinghofer, 2001). Activation of G proteins requires the initial dissociation of GDP, leading to an intermediate and transient nucleotide-free (apo) state. In all G proteins, the subsequent binding of GTP turns the G protein 'on' and causes two regions, defined as 'Switch I' and 'Switch II', to change conformation, which allows specific 'effector' proteins to interact and convey the signalling pathway. Hydrolysis of GTP to GDP eventuates in an 'off' state, reversing the structural changes with attenuation of downstream signalling, completing the G protein cycle (Sprang, 1997; Vetter and Wittinghofer, 2001).

Central to understanding G protein coupled signal transduction is the mechanism by which the dissociation of GDP is catalysed. For the heterotrimeric $G\alpha\beta\gamma$ proteins, the dissociation of GDP from the $G\alpha$ subunit is catalysed by activated membrane-bound G protein coupled receptors (GPCRs), which associate with the GDP-bound $G\alpha\beta\gamma$ and act as a guanine exchange factor (GEF) (Oldham *et al*, 2007; Oldham and Hamm, 2008). Recent studies have indicated that the GEF activity conferred by GPCRs is achieved by the modulation of structural changes in the G5 motif of the $G\alpha$ subunit, leading to a reduced affinity for GDP (Hamm *et al*, 1988; Johnston and Siderovski, 2007a, b; Scheerer *et al*, 2008). Further indication of the role played by the G5 motif is a $G\alpha_s$ mutant (Ala366Ser), clinically characterized by testotoxicosis (precocious puberty) in males due to an accelerated GDP release (Iiri *et al*, 1994). This mutation was mapped to the G5 motif and, in effect, it was proposed that the mutation mimics the accelerated dissociation of GDP normally induced by the agonist-activated GPCR. In structural studies of G proteins with bound GDP and GTP, the G5 motif has been shown to coordinate to the nucleotide base through a conserved hydrogen-bonding network (Sprang, 1997). However, a full understanding of the involvement of the G5 motif in GDP release requires structural characterization of the nucleotide-free transition state, a challenging feat due to its inherent instability in these systems (Sprang, 1997; Johnston and Siderovski, 2007a, b; Oldham and Hamm, 2008).

Prokaryotic uptake of ferrous iron (Fe^{2+}) has recently emerged as a G protein coupled process involving the membrane protein FeoB, which has possible evolutionary links to eukaryotic G protein coupled membrane processes (Marlovits *et al*, 2002; Hantke, 2003). FeoB is unique in that it includes an intracellular G protein directly fused to a polytopic membrane transport protein, separated by a short linker domain of unknown function (Marlovits *et al*, 2002; Daley *et al*, 2005) (Supplementary Figure S1). Mutational studies and sequence similarity between the G protein domain and the human oncogene p21-Ras and $G\alpha$ proteins have identified the G1–G4 signature motifs in FeoB, although the critical G5

*Corresponding author. Structural Biology Program, Centenary Institute, Locked Bag No. 6, Sydney, New South Wales 2042, Australia. Tel.: +61 2 956 56280; Fax: +61 2 956 56101;
E-mail: m.jormakka@centenary.org.au
[5]These authors contributed equally to this work
[6]Present address: Division of Biophysics, Department of Medical Biochemistry and Biophysics, Karolinska Institute, 171 77 Stockholm, Sweden

Received: 20 May 2009; accepted: 29 June 2009; published online: 23 July 2009

loop could not be assigned (Marlovits *et al*, 2002). Crucially, as with its eukaryotic counterparts, critical aspects regarding the regulation and mechanism of nucleotide exchange within FeoB remain unexplained. Furthermore, the nature of the coupling between the G protein and the membrane domain is still undetermined (Marlovits *et al*, 2002; Cartron *et al*, 2006; Eng *et al*, 2008). In nucleotide-coupled transporters (e.g. ABC transporters), the coupling occurs through structural changes catalysed by the nucleotide hydrolysis, whereas in channels (e.g. the cyclic nucleotide-gated ion channels), it is the binding of nucleotide that is associated with structural changes (Clayton *et al*, 2004; Hollenstein *et al*, 2007; Bocquet *et al*, 2009; Rees *et al*, 2009). Functional characterization has shown that FeoB has intrinsically slow GTP hydrolysis, which suggests that FeoB functions as a nucleotide-gated Fe^{2+} channel. However, previous studies have revealed intrinsically high GDP release rates, which would yield a constitutive 'on' (GTP bound) state in the Fe^{2+} influx-machinery. To reconcile this apparent conundrum, FeoB would require stringent regulation of GDP dissociation.

With a tethered G protein, reminiscent of mammalian Ras and Gαβγ, FeoB presents a unique opportunity to study the regulation of nucleotide exchange and the coupling between a G protein and its cognate membrane component. To address this, we have determined crystal structures of both the apo and GTP-bound form of the entire soluble N-terminal domain of FeoB. We have discovered that FeoB forms a trimer around a central cytoplasmic pore, which is closed in the apo structure and open in the GTP-bound structure. The linker domain of FeoB is proposed to act as an intrinsic effector, coupling GTP binding with pore opening. On the basis of these results, a gating model for G protein coupled Fe^{2+} transport is discussed. Importantly, unambiguous identification and structural characterization of the G5 signature motif reveals it to play a deciding role in GDP release.

Results

FeoB$^{1-270}$ assembles into a trimeric complex

On the basis of sequence and hydropathy analysis, we generated a construct composed of the entire hydrophilic domain (residues 1–270) of FeoB ($FeoB^{1-270}$) from *Escherichia coli*. With this construct, we pursued structural studies and initially obtained crystals of the apo (nucleotide free) $FeoB^{1-270}$. The model was refined to a resolution of 2.2 Å with R and R_{free} values of 22.5 and 28.7%. In addition, the non-hydrolyzable GTP analogue 5′[β,γ-imido]triposphate derivative mant-GMPPNP (mGTP) was used to form a stable $FeoB^{1-270}$–mGTP complex, which crystallized in the space-group $P2_1$. The structure was refined to 2.74 Å with R and R_{free} of 22.7 and 29.4%, respectively. There was no clear density for the C-terminal nine amino acids (residues 262–270), which have been omitted from all models. Data collection and refinement statistics are presented in Table I (see Supplementary Figure S2 for representative electron density map).

$FeoB^{1-270}$ crystallized in four space groups ($C2$ and $P2_1$ present work, $P2_12_12_1$ and $P3_1$ data not shown). In all crystal forms, the overall structure of $FeoB^{1-270}$ resembles a funnel generated by a non-crystallographic trimeric assembly, with approximate three-fold symmetry between protomers (Figure 1). The protomer to protomer interface (buried surface of $\sim$1280 Å^2) is mainly stabilized by hydrophobic interactions, although hydrogen bonds and salt bridges between residues in neighbouring molecules further stabilize the trimer (see Supplementary Figure S1). To test the biological relevance of the oligomer, we designed a double cysteine mutant (Ala158Cys and Ala254Cys) to form an intersubunit disulphide bond linking subunits together according to Yernool *et al* (2004) (Supplementary Figure S3). The double Cys mutant, when treated with Cu(II) (1,10-phenantroline)$_3$, forms a stable 88 kDa trimer, illustrating the same oligomeric state of $FeoB^{1-270}$ in solution (Supplementary Figure S3 and Materials and methods). In addition, purified wild-type protein was cross-linked with glutaraldehyde, which clearly illustrated formation of a trimer in solution (Supplementary Figure S3). As all previous GTPases reside as either monomer or hetero trimers, $FeoB^{1-270}$ represents the first homo trimer constellation structurally defined. The orientation of the trimer in relation to the inner membrane is predicted from the location of the C-termini (on convex side) and membrane topology analyses (Daley *et al*, 2005) to be such that the concave side faces the cytoplasm (Figure 1B; Supplementary Figure S4). The surface facing the membrane has a charge distribution resembling that of the soluble domain of CorA (Eshaghi *et al*, 2006) and the K^+ channel KirBac1.1 (Kuo *et al*, 2003), with a negatively charged centre and a positively charged rim (Supplementary Figure S4).

Structure of (apo) FeoB$^{1-270}$

The overall fold of the $FeoB^{1-270}$ monomer is divided into two distinct domains connected through a flexible linker sequence; an N-terminal GTP-binding domain (G protein, residues 1–166), and a C-terminal helical domain (residues 178–261; Figure 1C). The C-terminal domain forms a helical bundle followed by an extended α-helix, here designated as the 'valve helix' (residues 241–261; see Figure 1C). The valve helix terminates close to the centre of the trimer and is in an ideal position to regulate the Fe^{2+} translocation process. The entire helical domain is a new structural feature, not observed in other G proteins, and a search using DALI revealed no significant structural homologues, whereas BLAST indicated low-sequence conservation in this domain between FeoB proteins from other prokaryotic species (see Supplementary Figure S1). Previous biochemical data have indicated this domain to be functioning as a guanine dissociation inhibitor (Eng *et al*, 2008), although our structure indicates that the domain is situated too far away from the nucleotide-binding site for a direct involvement in inhibition of nucleotide release. The N-terminal G protein, on the other hand, exhibits a polypeptide fold similar to the core of other prokaryotic and eukaryotic GTPases, consisting of a seven-stranded β-sheet (β1–β7) surrounded by five α-helices (α1–α5; Figure 1C). The structural similarity between the G protein domain of $FeoB^{1-270}$ and other G proteins is illustrated by the r.m.s.d in Cα positions from their superimpositions; 1.83 Å for p21-Ras (114 Cα atoms, PDB code 5P21) and 1.63 Å for $G\alpha_{i1}$ (112 Cα atoms, PDB code 2G83; Supplementary Figure S5).

The four consensus elements, G1–G4, which are involved in GTP and Mg^{2+} binding in all G proteins (Bourne *et al*, 1991), are also present in FeoB (Supplementary Figure S1). In addition, the effector-binding regions recognized as Switch I (residues 25–40) and Switch II (residues 70–84)

Table I Data collection, phasing and refinement statistics for the Pb derivative, Native, mGTP-FeoB$^{1-270}$ and apo-FeoB$^{1-270}$ structures

	Pb derivative	Native	apo-FeoB$^{1-270}$	mGTP-FeoB$^{1-270}$
Data collection				
Space group	$P2_12_12_1$	$P2_12_12_1$	$C2$	$P2_1$
Cell dimensions				
a, *b*, *c* (Å)	47.7, 122.9, 134.5	47.4, 122.4, 134.7	146.1, 84.4, 66.2	76.0, 46.4, 120.1
α, β, γ (deg)	90, 90, 90	90, 90, 90	90, 108, 90	90, 95, 90
Wavelength (Å)	1.5418	0.9753	0.9793	0.9793
Resolution (Å)[a]	20–2.90 (3.06–2.90)	60–2.4 (2.53–2.4)	70–2.2 (2.32–2.2)	50–2.72 (2.82–2.72)
R_{merge}[a]	0.093 (0.270)	0.066 (0.248)	0.176 (0.459)	0.088 (0.421)
$I/\sigma I$[a]	7.0 (2.8)	8.6 (3.0)	3.3 (1.8)	14.3 (2.5)
Completeness (%)[a]	96.8 (83.4)	99.1 (99.4)	99.9 (99.9)	96.7 (82.0)
Redundancy	5.6	4.0	7.3	3.2

	apo-FeoB$^{1-270}$	mGTP-FeoB$^{1-270}$
Refinement		
PDB Code	3HYR	3HYT
Resolution (Å)[a]	72–2.20 (2.26–2.20)	45–2.74 (2.81–2.74)
No. reflections	36896	20674
R_{work}/R_{free}[a]	0.225/0.287 (0.322/0.361)	0.227/0.294 (0.316/0.423)
Residues included in the final model	A/B/C2-64, A/B/C71-260	A2-30, A40-64, A71-261, B2-30, B40-64, B71-260, C2-30, C40-63, C74-261
No. atoms		
Protein	5841	5722
Ligand/ion	0	129
Water	480	102
B-factors		
Protein	21.2	39.8
Ligand/ion		38.4
Water	21.3	25.3
r.m.s.d.		
Bond lengths (Å)	0.013	0.006
Bond angles (deg)	1.486	1.000
Ramachandran analysis[b]		
Favoured regions (%)	98.0	96.6
Allowed regions (%)	100.0	100.0
PDB accession code		

[a]Values in parentheses are for the highest-resolution shell.
[b]As assessed by MOLPROBITY ([10]).

are structurally analogous to those of other GTPases (Sprang, 1997). In the apo FeoB$^{1-270}$ structure, the Switch I region forms an extension to the central canonical β-sheet (β2), similar to the GDP-liganded structure of Ran, another G protein in the Ras superfamily (Scheffzek *et al*, 1995).

The G5 motif is, despite low sequence conservation, attributed to critical guanine base coordination (Sprang, 1997) and believed to be key to the GPCR catalysed nucleotide exchange in Gα subunits (Oldham *et al*, 2006; Oldham and Hamm, 2007, 2008). Previous attempts to clearly identify this motif in FeoB$^{1-270}$ by sequence alignments and mutational analysis were unsuccessful (Marlovits *et al*, 2002; Hantke, 2003; Eng *et al*, 2008). In our structure, the G5 motif can unambiguously be identified as residues (150)STRGRG(155) by superimposition with Gα and Ras. This reveals the G5 motif to be in a different position in the amino-acid sequence than suggested earlier (Marlovits *et al*, 2002; Hantke, 2003). Structural characterization of the G5 motif in the intermediate apo state is rare due to the inherent instability of this state (Sprang, 1997; Johnston and Siderovski, 2007a, b; Oldham and Hamm, 2008). However, in the apo structure of FeoB$^{1-270}$, the G5 motif is stabilized through a hydrogen bond between Ser150 and Asp123, and through a salt bridge formed between the G5 residue Arg154 and the conserved Glu99 in the neighbouring protomer (Figure 2A). The hydrogen bond between Ser150 and Asp123 is noteworthy, as Asp123 has been shown to be essential for GDP/GTP binding (Marlovits *et al*, 2002).

The structure of mGTP complex reveals conformational changes

To confirm the GTP binding properties of FeoB, we determined the structure of FeoB$^{1-270}$ bound to the non-hydrolysable GTP analogue mGTP. The structure of mGTP-FeoB$^{1-270}$ was refined to 2.74 Å resolution. Electron density clearly identified the position of a single mGTP molecule per protomer, and a putative Mg^{2+} ion bound adjacent to the γ-phosphate of mGTP (Supplementary Figure S2). The Mg^{2+}-binding site and mGTP coordination pattern mirror those found in other G proteins, including p21-Ras and Gα subunits (Wall *et al*, 1995; Sprang, 1997). The phosphate moieties of mGTP interact with the P-loop (G1; residues 10–18), particularly through Asn13, the hydroxyl group of Thr18, the amino group of Lys16, and backbone carbonyl oxygen and amine groups. The hydrophobic guanine group interacts with highly conserved residues in the G4 region, including Asn120 and Asp123, which form hydrogen bonds with the O6/N7, and N1/N2 atoms of mGTP, respectively (Figure 2B).

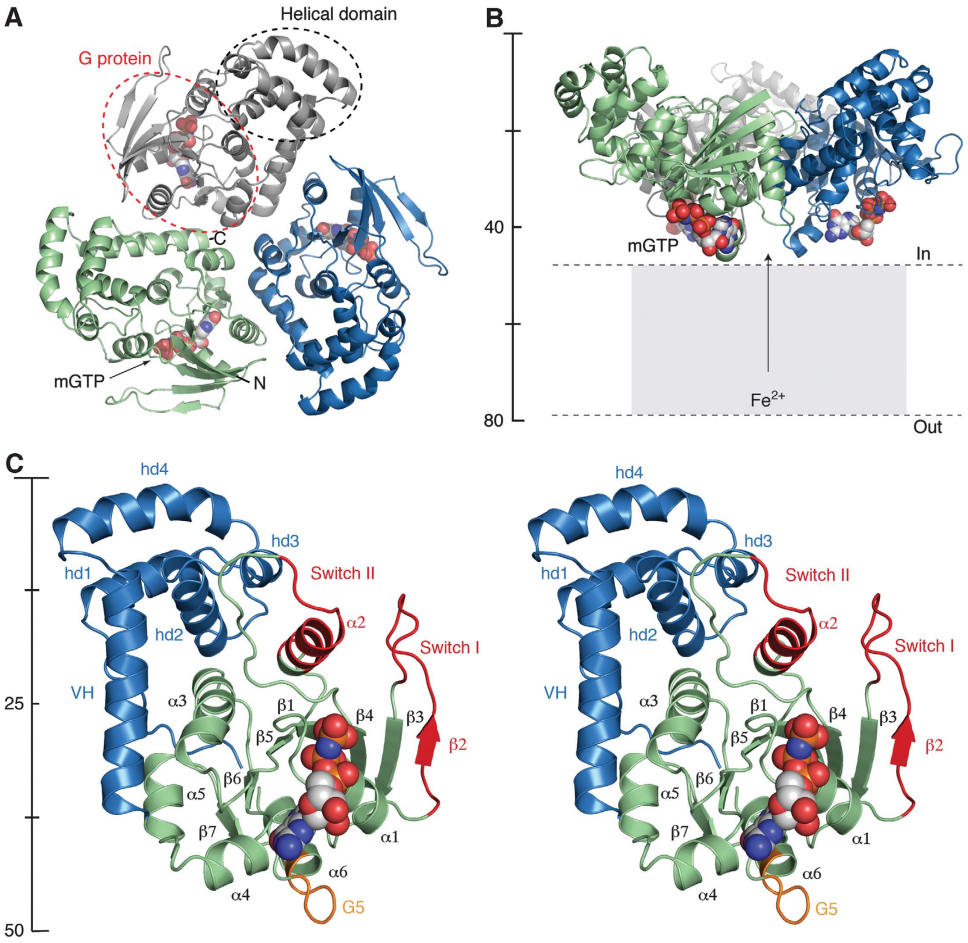

Figure 1 Overall structure of FeoB$^{1-270}$. (**A**) Ribbon representation of the trimer viewed from the intracellular space. Individual protomers are coloured in grey, green, and blue. Dotted lines indicate the spatial organization of the G protein and helical domain. (**B**) Side view of the trimer, with colours as in (A). The mGTP molecule is shown as space-fill. (**C**) Stereo view of one protomer. The N-terminal G protein and helical domain are illustrated in green and blue, respectively. The Switch regions are shown in red, and the G5 motif is depicted in orange. All structural figures were made using PyMOL (http://pymol.sourceforge.net).

In relation to the apo structure, one significant observation is a large structural change in the newly identified G5 motif. In the mGTP-FeoB$^{1-270}$ structure, this motif has shifted ~9 Å closer to the GTP-binding site, breaking the salt bridge between Arg154 and Glu99 and the hydrogen bond between Asp123 and Ser150 (Figure 2C). This 'in' conformation of the G5 motif is stabilized by hydrogen bonds between Thr151 (G5) and the N1 atom of mGTP, and between Ser150 (G5) and Gln22/Asn120. In addition, the 'in' state in the mGTP-liganded structure is likely further stabilized and dependent on the minor structural changes taking place in other motifs, including Switch I/Switch II, following mGTP binding.

Stopped-flow measurements corroborate the role of the G5 motif in GDP release

Comparison of the apo and mGTP-bound structures indicates that the conformational transition in the G5 motif has an important function in GDP release. To corroborate this hypothesis, we performed a structural comparison with the Gα_{i1} subunit mutant (Ala326Ser; PDB Entry code 1BH2), which is the corresponding mutant to the precocious puberty causing Gα_s Ala366Ser. Native FeoB$^{1-270}$ has a polypeptide sequence that mimics the Gα mutants with a Serine residue occupying the structurally equivalent position in the G5 motif (Gα_{i1} Ala326Ser versus FeoB$^{1-270}$ Ser150). As the Gα_s mutant has been characterized with an 80-fold acceleration in its rate constant of GDP release ($k_{off,GDP}$ 0.23 s^{-1}, compared with $k_{off,GDP}$ 0,003 s^{-1} in wt protein) (Iiri *et al*, 1994), we wanted to explore whether we could decelerate the GDP release in FeoB$^{1-270}$ by inversely mutating Ser150 to an Alanine residue. Consistent with the structural parallels, stopped-flow measurements confirmed native FeoB$^{1-270}$ to have an extremely high GDP release rate constant ($k_{off,GDP}$ 145 (±9) s^{-1}, 20°C; Table II) (Marlovits *et al*, 2002; Eng *et al*, 2008). Conversely, the Ser150Ala mutant showed drastically altered release rate constant ($k_{off,GDP}$ 10 (±0.1) s^{-1}, 20°C), consistent with our hypothesis that the G5 motif is involved in the rapid GDP release in native FeoB$^{1-270}$. To further investigate the relevance that the G5 'out' hydrogen-bonding network has on the GDP release rate, we also mutated Arg154 (Arg154Ala). As with the Ser150Ala mutant, the Arg154Ala protein shows a drastically decreased release rate constant ($k_{off,GDP}$ 19 (±0.5) s^{-1}, 20°C; Table II).

mGTP binding leads to the opening of a central cytoplasmic pore

All G proteins present an effector site on GTP binding; for Ras type G proteins and Gα subunits, the effector

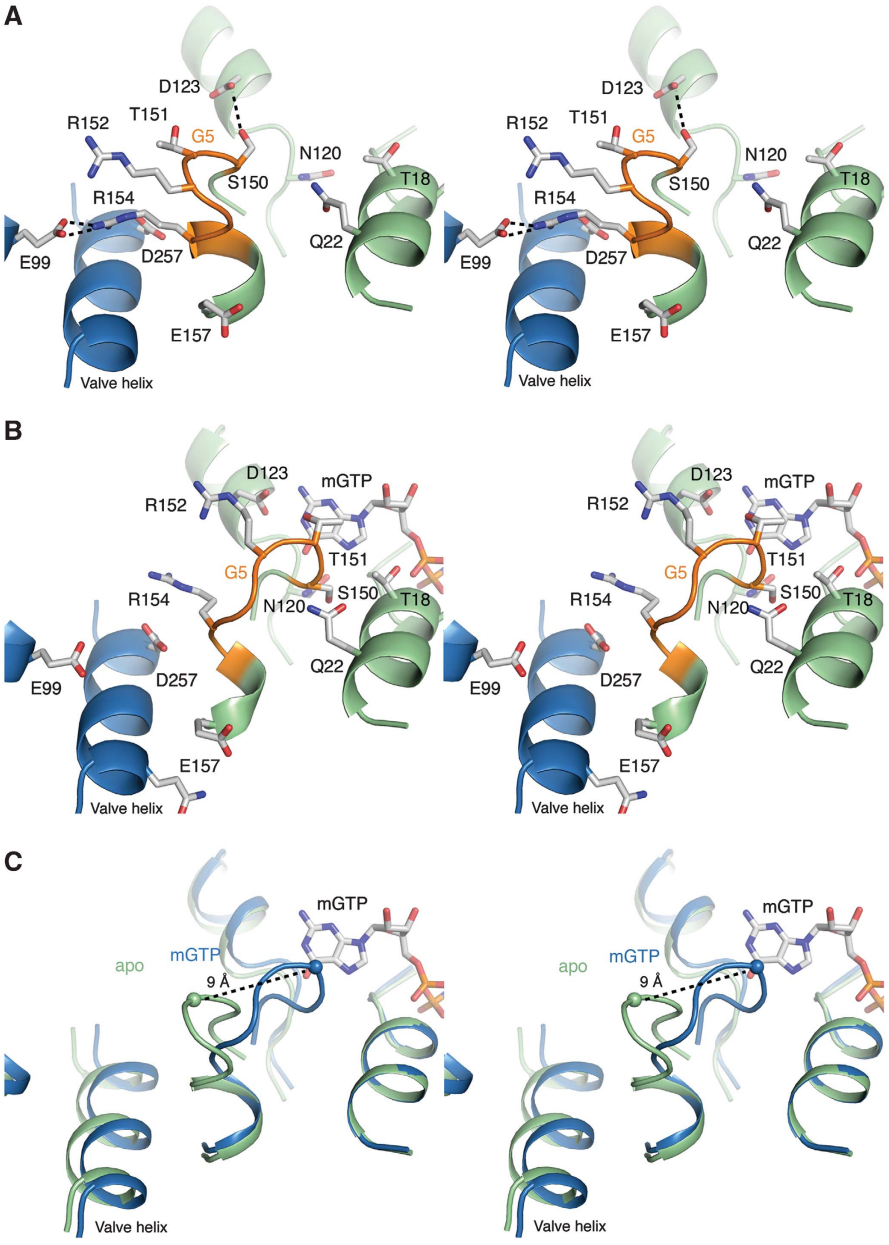

Figure 2 Stereo views of the G5 motif and mGTP-binding site. (**A**) Apo state. The G protein is shown in green, with the G5 motif highlighted in orange. The neighbouring protomer is shown in blue. An interprotomeric salt bridge between Arg154 and Glu99, and an intraprotomeric hydrogen bond between Asp123 and Ser150 stabilizes the G5 'out' state. (**B**) mGTP state. Contraction of the G protein after GTP binding leads to a high affinity G5 'in' state. In the transition, the salt bridge between Arg154 and Glu99, and hydrogen bond between Asp123 and Ser150, are broken. (**C**) Superimposition reveals a structural shift of ~9 Å in the Cα position of Thr151 between the 'in' and 'out' conformation.

Table II Rate constants for the association (k_{obs}) and dissociation (k_{off}) of mant-nucleotides with FeoB$^{1-270}$

Protein	Concentration (μM)	mGMPPNP k_{obs} s^{-1} (20°C)	mGMPPNP k_{off} s^{-1} (20°C)	mGDP $k_{off,GDP}$ s^{-1} (20°C)
FeoB$^{1-270}$	2.5	1.63		
	5	1.93	1.85	145 (±9)
	10	2.68		
	20	4.01		
	40	6.71		
S150A	5	3.87	1.77	10 (±0.1)
R154A	5	2.14	1.89	19 (±0.5)

association is through the active conformation of Switch I and Switch II (Spoerner *et al*, 2001; Tesmer *et al*, 2005; Sprang *et al*, 2007). In FeoB, the helical domain is situated in proximity to Switch II (Figure 1C), and structural changes in Switch II following mGTP binding are accompanied by observed disorder in the helical domain, indicating that the

helical domain is acting as an intrinsic effector. This structural change is transmitted to the valve helix, which in relation to the apo structure has shifted 1–2 Å away from the centre of the trimer.

Following this, a striking aspect of the trimeric mGTP-bound structure is that it forms a central cytoplasmic pore, about 20 Å in length and with a diameter of ~1.2 Å at the narrowest point (Figure 3). The cytoplasmic pore could facilitate gating and passage of un-hydrated Fe^{2+} ions (ionic radius of Fe^{2+} $\sim 0.76 \times 10^{-10}$ m) delivered from the transmembrane domain. In the apo structure (both *C*2 and $P2_12_12_1$ data), Glu133 is in a conformation that effectively blocks the pore (Figure 3A). However, the structural adaptation occurring on mGTP binding is accompanied by a change in the hydrogen-bonding pattern in the centre of the trimer interface. In the $FeoB^{1-270}$-mGTP structure, the Glu133 residue has a different conformation, which is stabilized by hydrogen bonds to the backbone amino group of Ile134 in the neighbouring molecule (Figure 3B). The driving force for the conformational change likely originates from mGTP binding, followed by small changes in the structure of the helical domain and the valve helix, which are ideally positioned to regulate the pore (Figure 3C).

Discussion

To delineate the complex structure/function relationships of channels or transporter proteins, the individual structural and functional domains are often studied in isolation. To this end, we solved the structures of the apo and mGTP-bound states of the soluble domain of FeoB. Our structural data provides, for the first time, anatomical information of a G protein, which is directly involved in the gating of membrane ion transport processes. A comparative analysis between the apo and mGTP-bound structures along with measured and known biochemical data, begin to reveal the mechanism for GDP release and gating of G protein coupled Fe^{2+} translocation.

Mechanism of GDP release

The structural changes recognized when the apo- and mGTP-$FeoB^{1-270}$ structures are compared have not been observed in other systems. In particular, the lack of an equivalent nucleotide-free (apo) structure for the heterotrimeric Gαβγ protein has left the mechanism of GDP release open to debate. As we have determined the structures of both apo and liganded states of $FeoB^{1-270}$, we can depict the structural transitions

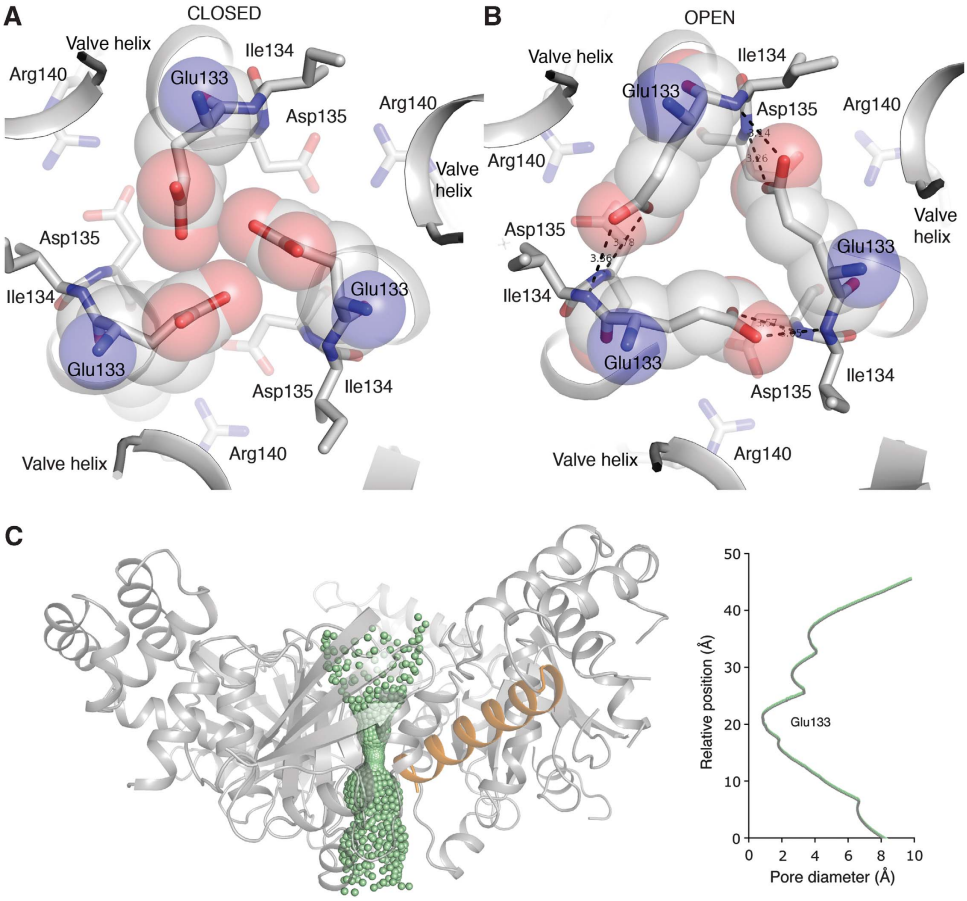

Figure 3 Details of the cytoplasmic gate. (**A**) Apo structure. View from the membrane side down the centre of the trimer. The trimer is stabilized through a salt bridge formed between Asp135 and Arg140 in neighbouring protomers. In the apo state, Glu133 is pointing to the centre, effectively closing the pore. (**B**) In the mGTP-bound structure, structural changes leads to a shift in the position of Cα atoms surrounding the centre of the trimer. This enables Glu133 to change conformation and form hydrogen bonds with mainchain N-atoms of Ile134. The new conformation leads to opening of a central cytoplasmic pore. (**C**) The pore diameter along the proposed cytoplasmic gate in the open state. The main site of constriction and gating (residue Glu133) is depicted. The valve helix from one protomer is shown in orange to illustrate its position in relation to the pore. The cytoplasmic pore was generated using HOLE (Smart *et al*, 1993).

driving GDP release. A rapid GDP release rate for FeoB$^{1-270}$ indicates that the G5 motif has an inherent propensity to switch to a stable 'out' state, a state in which the affinity for GDP is nominal. This propensity is likely due to the ability of residues in the G5 motif to participate in stabilizing interactions (salt bridges and hydrogen bonds) when in the 'out' conformation. This was corroborated by our stopped-flow experiments, which revealed altered GDP release rates when the residues involved in the stabilizing interactions were mutated. Despite the reduced rate of the GDP release in the mutated protein, it remains high when compared with Ras type G proteins and G$\alpha\beta\gamma$ proteins. This intrinsically elevated GDP release rate could be due to other residues in the G5 loop, such as Gly153 or Gly155, which could act as 'hinge' residues and allow for a highly flexible structure. In addition, the movement of the G5 loop could be regulated by an as-yet-unidentified factor to slow down GDP release.

From this we propose that G$\alpha\beta\gamma$ proteins could harbour a similar structural flexibility as observed in FeoB$^{1-270}$ and that the elusive apo state in the activated GPCR/G$\alpha\beta\gamma$ complex includes an 'out' conformation of the G5 motif. In support of the hypothesis that Gα subunits have a conformational two-way G5 motif, are previous studies of the GPCR/G$\alpha\beta\gamma$ interactions that have indicated that conformational changes in the G5 motif are key for GDP release (Hamm *et al*, 1988; Oldham and Hamm, 2008; Scheerer *et al*, 2008). In addition, recent NMR analysis of a receptor-associated (apo) Gα revealed the nucleotide-free form to represent a structurally dynamic intermediate state (Abdulaev *et al*, 2006).

Mechanism of G protein coupled gating

It is unclear from the structures presented here whether the pore in the mGTP-bound state of FeoB$^{1-270}$ has reached maximum aperture, or whether the structure represents a transition state. However, the structural data presented here in concert with published functional data facilitates a novel and simple mechanism for G protein coupled gating of Fe^{2+} membrane translocation; (i) binding of GTP-Mg^{2+} is coupled to structural transitions in Switch I and Switch II; (ii) the 'active' conformation of the Switch regions causes the helical domain, which acts as an intrinsic effector, to move towards the presented effector site (Switch II); (iii) the shift in the helical domain drives a lateral movement of the valve helix, which leads to the opening of a central cytoplasmic pore, allowing Fe^{2+} to enter the cell through the transmembrane domain (see Figure 3; Supplementary Figure S6); (iv) hydrolysis of GTP to GDP leads to a concerted relaxation of the Switch regions, release of the helical domain from the effector site, and closing of the pore.

Materials and methods

Expression and purification of FeoB$^{1-270}$

FeoB$^{1-270}$ was sub-cloned from a full-length *E. coli* FeoB construct (Daley *et al*, 2005) and inserted into a pGEX4-T1 vector (GE Healthcare Life Sciences) and expressed as a fusion protein with glutathion S-transferase (GST). Native and mutant protein was purified using GST affinity chromatography according to the manufacturer's protocol. The GST moiety was removed by thrombin cleavage and the protein was polished by size exclusion chromatography (Superdex 75; GE Healthcare Life Sciences). Purified protein was buffer exchanged to 20 mM Tris pH 8.0 and concentrated to 20 mg ml^{-1}.

Crystallization and X-ray data collection

Crystals of native FeoB$^{1-270}$ ($\sim$20 mg ml^{-1}) were grown by mixing protein and reservoir solution (30% PEG 400, 100 mM $MgCl_2$, 0.1 M MES pH 6.5) in a 2:1 ratio using the hanging-drop technique. Crystals appeared after 48 h at 20°C and grew to maximal dimensions of $100 \times 100 \times 70$ μm within a week. Crystals of native FeoB$^{1-270}$ grew in space group $P2_12_12_1$, whereas crystals of Se-Met labelled protein (apo-FeoB$^{1-270}$) crystallized in *C*2. A nucleotide-bound protein was obtained by co-crystallizing the native FeoB$^{1-270}$ protein in the presence of 1 mM mGTP. Crystals appeared in the same reservoir solution as the native protein, although crystals grew in spacegroup $P2_1$. The analogue GMPPMP was also used for co-crystallization trials, although the mGTP provided the highest resolution structure. A Pb-derivative crystal was prepared by soaking a crystal of the native protein in a solution containing trimethyllead acetate (5 mM) for 1 h, before data collection.

X-ray data were collected from native, mGTP-FeoB$^{1-270}$, and Se-Met labelled apo-FeoB$^{1-270}$ crystals using a MARmosaic 300 detector at beamline ID23 B/D at the Advanced Photon Source (APS, Chicago). Data from heavy atom soaked crystals (Pb-derivative) were collected on a Rigaku MicroMax 007HF Cu rotating anode X-ray generator with Osmic VariMax HF focusing optics and a MAR345 Image Plate detector. All image data were collected at 100 K and processed using Denzo & Scalepack (Otwinowski *et al*, 1997) or Mosflm (Leslie, 1992) and Scala (Collaborative Computational Project, Number 4, 1994). Cell dimensions and data collection statistics are presented in Table I and Supplementary data.

Structure determination and refinement of apo and liganded FeoB$^{1-180}$

The structure of FeoB$^{1-270}$ was determined by SIRAS phasing, using data from Pb-derivatized and native crystals. Heavy atom sites were determined with SHELXD (Sheldrick, 2008) and refined with SHARP (Bricogne *et al*, 2003). SIRAS phases to 2.9 Å were applied to the native data set and extended to 2.2 Å using three-fold averaging, solvent fattening and histogram mapping in DM (Collaborative Computational Project, Number 4, 1994). The atomic model was built using the programs O (Jones *et al*, 1991) and COOT (Emsley and Cowtan, 2004). During the model building process, it was rapidly recognized that significant regions of the FeoB$^{1-270}$ structure were disordered in the native crystals. The coordinates of the preliminary model were therefore used as a molecular replacement model to determine the structure of FeoB$^{1-270}$ in crystals grown from the Se-Met labelled protein (space group *C*2), using PHASER. Model building was completed using this data and refinement was carried out using REFMAC5 (Murshudov *et al*, 1997) (with TLS) and PHENIX (Zwart *et al*, 2008). As the data from the Se-Met labelled protein produced the most complete model, this structure will hereafter be referred to as apo-FeoB$^{1-270}$. The coordinates of the resulting apo-FeoB$^{1-270}$ model were used as a molecular replacement model to determine the structure of mGTP-FeoB$^{1-270}$ using PHASER (McCoy *et al*, 2007). The coordinates of both the apo-FeoB$^{1-270}$ and mGTP-FeoB$^{1-270}$ structures have been deposited in the Protein Data Bank with accession codes 3HYR and 3HYT, respectively.

GTPase activity measurements

GTP hydrolysis assay was performed using a Malachite Green Phosphate Assay (BioAssay Systems) that provides colorimetric detection of inorganic phosphate. FeoB$^{1-270}$ (2 μM) in Tris buffer (20 mM Tris pH 8.0, 100 mM NaCl) was incubated for 8–20 h with GTP (20 μM) at 25°C. Reactions were terminated on addition of malachite green reagent (40 μl) and A_{620} was measured after 30 min to monitor hydrolysis. Appropriate controls were performed to ensure that there was no background interference from the reaction components.

Mutagenesis

The plasmid pGEX-4T1/FeoB$^{1-270}$ was used to generate expression vectors with single amino-acid mutations (S150A and R154A) and one double mutant (A158C/A254C), by using Stratagene's Quick-Change site-directed mutagenesis kit. Mutants were expressed and purified as the wt protein.

Cross-linking

Purified $FeoB^{1-270}$ double mutant, A158C/A254C, was concentrated to $\sim 4\,mg\,ml^{-1}$ and left at 4°C for 3 days to allow for assembly of oligomer. For the cross-linking reaction, Cu(II) (1,10-phenantroline)$_3$ was prepared by adding fresh mixture of equal volumes of 0.5 mM $CuSO_4$ and 1.5 mM 1,10-phenantroline prepared in ethanol and diluted 1 in 10 with 1 M sodium citrate (pH 5.6). 1 mM of Cu(II) (1,10-phenantroline)$_3$ was added to gel-filtration fractions of $FeoB^{1-270}$ trimer and reactions were carried out at room temperature for 1 h. The samples were analysed by SDS–polyacrylamide gel electrophoresis (PAGE) under non-reducing conditions. The protein bands were identified and molecular mass of protein in solution was determined by mass spectrometry (SUPRU, University of Sydney).

Purified wild-type $FeoB^{1-270}$ was also cross-linked with glutaraldehyde (0.01 mM) at 25°C for 30 min and reactions were quenched using 150 mM Tris pH 7.5. Cross-linked protein was subsequently evaluated by SDS–PAGE.

Stopped-flow fluorescence assay

A stopped-flow based assay was performed to determine binding and release of fluorescent nucleotides in wt $FeoB^{1-270}$ and the S150A/Arg154Ala mutants as described (Marlovits *et al*, 2002). Briefly, to determine release rate constants, 10 mM of native $FeoB^{1-270}$ or mutant protein was incubated with 0.5 mM of mGDP in stopped-flow buffer (20 mM MES, pH 6.5, 100 mM NaCl, 10 mM $MgCl_2$,) for 30 min at room temperature. Equal volumes of the protein-mGDP mix and 1 mM GTP in stopped-flow buffer were rapidly mixed into a 22.5 μl optical cell of a pneumatically driven stopped-flow apparatus (SF-61, Hi-Tech Scientific Ltd., Salisbury, UK). The mant group was excited using the 355 nm line of a 100 W short arc mercury lamp (Osram, Berlin, Germany) and the fluorescence was monitored at right angles to the incident light beam using an R928 multialkali side-on photomultiplier. The fluorescence was collected at wavelengths $\geqslant$400 nm by using a GG400 glass cut-off filter (Schott, Mainz, Germany) in front of the photomultiplier. Similarly, observed binding rate constants were determined by rapidly mixing 2.5–40 mM $FeoB^{1-270}$ or 5 mM mutant protein with 0.5 mM mGMPPNP in the stopped-flow apparatus. All data reported are averages of 7–10 independent experimental traces performed under identical conditions. Reactions were performed at 20°C. At this temperature the rate constants $k_{obs,mGDP} > 1000\,s^{-1}$ were obtained, indicating that GDP binding and dissociation occurred on a time scale faster than what can be reliably measured by stopped-flow.

Supplementary data

Supplementary data are available at *The EMBO Journal* Online (http://www.embojournal.org).

Acknowledgements

This study was supported by the Australian Research Council (ARC; DP0666970 to MJ). MR was a recipient of the Australian Research Council Linkage Fellowship (LX0881956) and supported by Stiftelsen Bengt Lundqvist Minne. MJM was supported by a Cancer Institute of NSW Career Development Fellowship. Data collection was done at the Advanced Photon Source (APS). We acknowledge the support of S Corcoran, N Venugopolan, and M Becker at GM/CA-CAT, for scientific support and assistance with data collection. GM/CA-CAT beamline (ID23) is supported by the US National Cancer Institute and the US National Institute of General Medical Science. Visits to APS were supported by the Australian Nuclear Science Technology Organization (ANSTO). This research was facilitated by access to the Sydney University Proteome Research Unit, established under the Australian Government's Major National Research Facilities program and supported by the University of Sydney. G von Heijne is acknowledged for supplying the FeoB-GFP vector and B Crossett for mass spectrometry. We thank Jeff Abramson and Gunnar von Heijne for critical assessment of the paper.

Conflict of interest

The authors declare that they have no conflict of interest.

References

Abdulaev NG, Ngo T, Ramon E, Brabazon DM, Marino JP, Ridge KD (2006) The receptor-bound 'empty pocket' state of the heterotrimeric G-protein alpha-subunit is conformationally dynamic. *Biochemistry* **45:** 12986–12997

Bocquet N, Nury H, Baaden M, Le Poupon C, Changeux JP, Delarue M, Corringer PJ (2009) X-ray structure of a pentameric ligand-gated ion channel in an apparently open conformation. *Nature* **457:** 111–114

Bourne HR, Sanders DA, McCormick F (1991) The GTPase superfamily: conserved structure and molecular mechanism. *Nature* **349:** 117–127

Bricogne G, Vonrhein C, Flensburg C, Schiltz M, Paciorek W (2003) Generation, representation and flow of phase information in structure determination: recent developments in and around SHARP 2.0. *Acta Crystallogr D Biol Crystallogr* **59:** 2023–2030

Cachero TG, Morielli AD, Peralta EG (1998) The small GTP-binding protein RhoA regulates a delayed rectifier potassium channel. *Cell* **93:** 1077–1085

Cartron M, Maddocks S, Gillingham P, Craven C, Andrews S (2006) Feo—transport of ferrous iron into bacteria. *BioMetals* **19:** 143–157

Clayton GM, Silverman WR, Heginbotham L, Morais-Cabral JH (2004) Structural basis of ligand activation in a cyclic nucleotide regulated potassium channel. *Cell* **119:** 615–627

Collaborative Computational Project, Number 4 (1994) The CCP4 suite: programs for protein crystallography. *Acta Crystallogr D Biol Crystallogr* **50:** 760–763

Daley DO, Rapp M, Granseth E, Melen K, Drew D, von Heijne G (2005) Global topology analysis of the Escherichia coli inner membrane proteome. *Science* **308:** 1321–1323

Davis IW, Leaver-Fay A, Chen VB, Block JN, Kapral GJ, Wang X, Murray LW, Arendall WB, Snoeyink J, Richardson JS, Richardson DC (2007) MolProbity: all-atom contacts and structure validation for proteins and nucleic acids. *Nucleic Acids Res* **35:** W375–W383

Emsley P, Cowtan K (2004) Coot: model-building tools for molecular graphics. *Acta Crystallogr D Biol Crystallogr* **60:** 2126–2132

Eng ET, Jalilian AR, Spasov KA, Unger VM (2008) Characterization of a novel prokaryotic GDP dissociation inhibitor domain from the G protein coupled membrane protein FeoB. *J Mol Biol* **375:** 1086–1097

Eshaghi S, Niegowski D, Kohl A, Molina DM, Lesley SA, Nordlund P (2006) Crystal structure of a divalent metal ion transporter CorA at 2.9 Angstrom resolution. *Science* **313:** 354–357

Finlin BS, Correll RN, Pang C, Crump SM, Satin J, Andres DA (2006) Analysis of the complex between Ca2 + channel beta-subunit and the Rem GTPase. *J Biol Chem* **281:** 23557–23566

Hamm HE, Deretic D, Arendt A, Hargrave PA, Koenig B, Hofmann KP (1988) Site of G protein binding to rhodopsin mapped with synthetic peptides from the alpha subunit. *Science* **241:** 832–835

Hantke K (2003) Is the bacterial ferrous iron transporter FeoB a living fossil? *Trends Microbiol* **11:** 192–195

Hollenstein K, Dawson RJ, Locher KP (2007) Structure and mechanism of ABC transporter proteins. *Curr Opin Struct Biol* **17:** 412–418

Iiri T, Herzmark P, Nakamoto JM, van Dop C, Bourne HR (1994) Rapid GDP release from Gs alpha in patients with gain and loss of endocrine function. *Nature* **371:** 164–168

Johnston CA, Siderovski DP (2007a) Receptor-mediated activation of heterotrimeric G-proteins: current structural insights. *Mol Pharmacol* **72:** 219–230

Johnston CA, Siderovski DP (2007b) Structural basis for nucleotide exchange on Gαi subunits and receptor coupling specificity. *Proc Natl Acad Sci* **104:** 2001–2006

Jones TA, Zou JY, Cowan SW, Kjeldgaard M (1991) Improved methods for building protein models in electron density maps and the location of errors in these models. *Acta Crystallogr A* **47** (Pt 2)**:** 110–119

Karnoub AE, Weinberg RA (2008) Ras oncogenes: split personalities. *Nat Rev Mol Cell Biol* **9:** 517–531

Kuo A, Gulbis JM, Antcliff JF, Rahman T, Lowe ED, Zimmer J, Cuthbertson J, Ashcroft FM, Ezaki T, Doyle DA (2003) Crystal structure of the potassium channel KirBac1.1 in the closed state. *Science* **300:** 1922–1926

Leslie AGW (1992) Recent changes to the MOSFLM package for processing film and image plate data. *Joint CCP4 + ESF-EAMCB Newslett Protein Crystallogr* **26:** 11–20

Marlovits TC, Haase W, Herrmann C, Aller SG, Unger VM (2002) The membrane protein FeoB contains an intramolecular G protein essential for Fe(II) uptake in bacteria. *Proc Natl Acad Sci USA* **99:** 16243–16248

McCoy AJ, Grosse-Kunstleve RW, Adams PD, Winn MD, Storoni LC, Read RJ (2007) Phaser crystallographic software. *J Appl Crystallogr* **40:** 658–674

Murshudov GN, Vagin AA, Dodson EJ (1997) Refinement of macromolecular structures by the maximum-likelihood method. *Acta Crystallogr D Biol Crystallogr* **53:** 240–255

Oldham WM, Hamm HE (2007) How do receptors activate G proteins? In *Mechanisms and Pathways of Heterotrimeric G Protein Signaling*, Sprang SR (ed) pp 67–93. San Diego: Academic Press

Oldham WM, Hamm HE (2008) Heterotrimeric G protein activation by G-protein-coupled receptors. *Nat Rev Mol Cell Biol* **9:** 60–71

Oldham WM, Van Eps N, Preininger AM, Hubbell WL, Hamm HE (2006) Mechanism of the receptor-catalyzed activation of heterotrimeric G proteins. *Nat Struct Mol Biol* **13:** 772–777

Oldham WM, Van Eps N, Preininger AM, Hubbell WL, Hamm HE (2007) Mapping allosteric connections from the receptor to the nucleotide-binding pocket of heterotrimeric G proteins. *Proc Natl Acad Sci USA* **104:** 7927–7932

Otwinowski Z, Minor W, Charles W, Carter J (1997) Processing of X-ray diffraction data collected in oscillation mode. In *Methods in Enzymology Macromolecular Crystallography Part A*, pp 307–326. San Diego: Academic Press

Rees DC, Johnson E, Lewinson O (2009) ABC transporters: the power to change. *Nat Rev Mol Cell Biol* **10:** 218–227

Schaafsma D, Roscioni SS, Meurs H, Schmidt M (2008) Monomeric G-proteins as signal transducers in airway physiology and pathophysiology. *Cell Signal* **20:** 1705–1714

Scheerer P, Park JH, Hildebrand PW, Kim YJ, Krausz N, Choe H, Hofmann KP, Ernst OP (2008) Crystal structure of opsin in its G-protein-interacting conformation. *Nature* **455:** 497–502

Scheffzek K, Klebe C, Fritz-Wolf K, Kabsch W, Wittinghofer A (1995) Crystal structure of the nuclear Ras-related protein Ran in its GDP-bound form. *Nature* **374:** 378–381

Sheldrick GM (2008) A short history of SHELX. *Acta Crystallogr A* **64:** 112–122

Smart OS, Goodfellow JM, Wallace BA (1993) The pore dimensions of gramicidin A. *Biophys J* **65:** 2455–2460

Spoerner M, Herrmann C, Vetter IR, Kalbitzer HR, Wittinghofer A (2001) Dynamic properties of the Ras switch I region and its importance for binding to effectors. *Proc Natl Acad Sci USA* **98:** 4944–4949

Sprang SR (1997) G protein mechanisms: insights from structural analysis. *Annu Rev Biochem* **66:** 639–678

Sprang SR, Chen Z, Du X (2007) Structural basis of effector regulation and signal termination in heterotrimeric G[alpha] proteins. In *Mechanisms and Pathways of Heterotrimeric G Protein Signaling*, Sprang SR (ed) pp 1–65. San Diego: Academic Press

Tesmer VM, Kawano T, Shankaranarayanan A, Kozasa T, Tesmer JJG (2005) Snapshot of activated G proteins at the membrane: the Galphaq-GRK2-Gbetagamma complex. *Science* **310:** 1686–1690

Vetter IR, Wittinghofer A (2001) The guanine nucleotide-binding switch in three dimensions. *Science* **294:** 1299–1304

Wall MA, Coleman DE, Lee E, Iñiguez-Lluhi JA, Posner BA, Gilman AG, Sprang SR (1995) The structure of the G protein heterotrimer Gi[alpha]1[beta]1[gamma]2. *Cell* **83:** 1047–1058

Yernool D, Boudker O, Jin Y, Gouaux E (2004) Structure of a glutamate transporter homologue from Pyrococcus horikoshii. *Nature* **431:** 811–818

Zwart PH, Afonine PV, Grosse-Kunstleve RW, Hung LW, Ioerger TR, McCoy AJ, McKee E, Moriarty NW, Read RJ, Sacchettini JC, Sauter NK, Storoni LC, Terwilliger TC, Adams PD (2008) Automated structure solution with the PHENIX suite. *Methods Mol Biol* **426:** 419–435